

Original Article

# Hybrid Metaheuristics with Deep Learning-Assisted Parkinson's Disease Detection and Classification

N. Navaneetha<sup>1</sup>, T. Suresh<sup>2</sup>, V. Sathiyasuntharam<sup>3</sup>

<sup>1,2</sup>Department of CSE, Annamalai University, Chidambaram, Tamil Nadu, India.

<sup>3</sup>CSE - Cyber Security, CMR Engineering College, Hyderabad, Telangana, India.

<sup>2</sup>Corresponding Author : [sureshaucse@gmail.com](mailto:sureshaucse@gmail.com)

Received: 04 February 2025

Revised: 06 March 2025

Accepted: 07 April 2025

Published: 29 April 2025

**Abstract** - Parkinson's Disease (PD) is a chronic neurological disorder that advances gradually, with signs often resembling those of other conditions. Timely detection and diagnosis of PD are crucial for giving the appropriate treatment, assisting patients in maintaining their health and improving their quality of life. These disease signs have been described as slowness in activities, muscle rigidity, tremors, and balancing with other psychiatric signs. Handwritten health records are the main devices that support PD recognition and evaluation. Many Machine Learning (ML) methodologies have been discovered for the early recognition of PD. However, many handcrafted feature extractor techniques mainly suffer from lower-performance accuracy problems. Therefore, Deep Learning (DL) models are widely used to analyse medical data. In this view, this study presents a Hybrid Meta-heuristics with DL Assisted PD Detection and Classification (HMDL-PDDC) technique. The HMDL-PDDC technique follows the hybrid metaheuristics-based Feature Selection (FS) design with an optimum DL method for recognizing and identifying PD. In the HMDL-PDDC technique, feature subsets are selected using an Improved Salp Swarm Algorithm (ISSA). Besides, the Kernel-based Deep Elman Neural Networks (KDENNs) technique is exploited to detect and identify PD. Moreover, the hyperparameter selection of the KDENN model is performed by an Object-Oriented Programming Optimization Algorithm (OOPOA) technique. The experimentation outcomes of the HMDL-PDDC model are examined under four datasets using a set of measures. The experimental assessment of the HMDL-PDDC technique illustrated superior accuracy values of 93.98%, 94.97%, 98.71% and 97.10% over existing models.

**Keywords** - Parkinson's Disease, Metaheuristics, Deep learning, Hyperparameter tuning, Salp Swarm algorithm.

## 1. Introduction

PD is a progressive neurological condition that has worsened over time, instigated by the early degeneration of dopamine-generating neurons in the substantia nigra region [1]. This degeneration primarily arises in the dorsal striatum and develops to the ventral part due to the spreading of such disease. The caudate and putamen nucleus that built the striatum is accountable for controlling numerous cognitive and motor functions. In PD, dopamine metabolism creates a higher level of reactive-oxygen contents, resulting in improved iron contents that will damage the cell constituents and harm the cerebral functions [2]. The degradation in dopaminergic paths is related to PD signs, with the reduction of dopaminergic neurons inducing non-motor and motor indications. Motor signs comprise slow movement, trouble walking, tremors, and stiffness, whereas the non-motor indications include examples such as sleep disorders, psychosis, depression, genitourinary problems, and accidents [3]. If 60% of dopaminergic neurons exist, these indications will be evident, and these are related to ageing factors, leading to reduced life quality. For the recognition of PD at an earlier

phase, most medical specialists must depend upon significant signs, namely complex walking, keeping bodily balancing, and shaking [4]. Accordingly, the research workers are considering approaches to recognize these non-motor indications as soon as possible to decrease the disease's growth. This is where ML determines the advantages [5].

Recently, developments in ML methods and the accessibility of large-scale databases have initiated novel possibilities for the automatic recognition of PD by employing different types of data comprising voice recordings [6]. ML-based PD recognition techniques can also be non-invasive, inexpensive, and simply scalable. A voice recording is gathered by employing normally obtainable devices like smartphones, which creates an accessible and suitable tool for monitoring and screening PD [7]. Various researchers have explored the field of PD identification, attaching voice data as an analytic indicator. However, a prominent gap is the restricted sizes and variety of the databases utilized in several previous kinds of research. This limitation complicates the consistency and applicability of the resulting classification



techniques [8]. This research work builds an essential involvement in the field by decidedly overcoming this problem over the application. Another gap is the lack of all-inclusive FS techniques utilized in PD classification. Although a few efforts have been made to implement FS methods, this consideration proceeds by presenting a new integration of filter FS with genetic selection and ensemble learning [9]. PD is a progressive neurological disorder with varied symptoms, making early detection challenging. Conventional diagnostic methods often depend on expert interpretation and invasive procedures, leading to delays in treatment. There is a growing requirement for effectual tools that enable early detection. By incorporating hybrid metaheuristics and DL, this study aims to enhance the accuracy and speed of PD detection, improving patient outcomes and healthcare efficiency [10].

This study presents a Hybrid Meta-heuristics with DL Assisted PD Detection and Classification (HMDL-PDDC) technique. The HMDL-PDDC technique follows the hybrid metaheuristics-based Feature Selection (FS) design with an optimum DL method for recognizing and identifying PD. In the HMDL-PDDC technique, feature subsets are selected using an Improved Salp Swarm Algorithm (ISSA). Besides, the Kernel-based Deep Elman Neural Networks (KDENNs) technique is exploited to detect and identify PD. Moreover, the hyperparameter selection of the KDENN model is performed by an Object-Oriented Programming Optimization Algorithm (OOPOA) technique. The experimentation outcomes of the HMDL-PDDC model are tested using a set of measures. The key contribution of the HMDL-PDDC model is given below.

- The HMDL-PDDC method utilizes a metaheuristics-based feature selection approach to detect the most relevant features from extensive datasets. This process enhances the capability of the technique to concentrate on critical data points, improving both its accuracy and efficiency. Choosing only the most crucial features mitigates complexity while maintaining high performance.
- The HMDL-PDDC technique employs the ISSA model to optimize feature subset selection, focusing on detecting the most crucial variables for PD detection. This results in mitigated dimensionality, improving computational efficiency while preserving critical data. The ISSA-based approach improves model performance by choosing only the most relevant features for accurate prediction.
- The HMDL-PDDC approach integrates the KDENN method to enhance feature representation and enable DL-based PD detection. By capturing intrinsic patterns and relationships in the data, KDENNs improve the accuracy of PD recognition. This approach effectually improves the capability of the method to detect PD with higher precision.
- The HMDL-PDDC methodology implements the OOPOA model for fine-tuning the model's hyperparameters, ensuring optimal performance in PD

detection. By efficiently adjusting key parameters, OOPOA assists in achieving improved accuracy and precision in predictions. This tuning process improves the overall efficiency of the method in recognizing PD.

- The novelty of the HMDL-PDDC approach stems from its unique integration of advanced metaheuristic-based feature selection, DL, and optimization methods for model tuning. This incorporation not only improves the accuracy and efficiency of the method but also addresses the complexities of PD detection. By utilizing these innovative approaches, the model presents a more robust, adaptable, and precise solution for recognizing PD compared to conventional methods.

## 2. Literature Works

Dharani and Thamilselvan [11] developed a chronological smart sunflower optimizer algorithm (CSSFOA) model. The Gaussian Filter (GF) and CSFOA are utilized for pre-processing and FS. This regarded the features through the method of Bray-Curtis's distance. The ZF-Net architecture performs the PD classification. In [12], the Adaptive Crow Search Algorithm (ACSA) and DL-assisted optimum FS model were projected. This method was the hybrid of CSA and DL Stack Sparse Autoencoder (SSAE)-NN. The ACSA method was utilized to determine the crunched feature vectors. Besides, SSAE with seven hidden layers (HLs) produces the compacted feature vectors. The authors [13] presented an improved sailfish optimizer algorithm with DL (ISFO-DL) method. This method employs the metaheuristic ISFO and DL techniques. The ISFO method was mainly employed to develop optimum feature subsets with a Fitness Function (FF) of maximal identification accuracy.

Furthermore, the Rat Swarm Optimizer (RSO) with the Bidirectional Gated Recurrent Unit (BiGRU) is used to classify. In [14], a method to classify PD by MRI brain imageries was developed. Initially, the min-max normalization technique, followed by noise elimination from the input imageries through a Median Filter (MF), is utilized. Also, the Dense-UNet is used for segmentation. The Deep Residual CNN (DRCNNs) with the Enhanced Whale Optimizer Algorithm (EWOA) model is used for classification. Chen et al. [15] utilized the DCNNs technique. The Chimp Optimizer Algorithm (ChOA) is used to choose the optimum structure of DCNN mechanically. Also, three ChOA-based models are used. An IPA-based encoding model for the DCNN layer utilizing Chimp Vectors (CVs) was initially made. Moreover, a layer of Enfeebled with definite CV sizes is used for variable-length DCNNs.

Pragadeeswaran and Kannimuthu [16] proposed an Adaptive Intelligent Polar Bear (AIPB) Optimizer-Quantized Contempo Neural Networks (QCNNs) approach. Where the Determinate Haar Wavelet (DHW) transformer method is utilized for pre-processing. The Statistical Time Frequency

Renyi (STFR) method is employed for extraction. Then, the AIPB-optimized methodology is implemented for feature extraction. Then, the QCNN model is employed for a forecast. Sharanyaa et al. [17] develop a method to identify PD utilizing voice signals. After FS, an exponential Delta-Amplitude Modulation Spectrogram (AMS) is created by uniting Exponential Weighted Moving Average (EWMA) and delta-AMS techniques. The FS is completed by utilizing the projected Squirrel Search Water Algorithm (SSWA), which was created by merging the Water Cycle Algorithm (WCA) with the Squirrel Search Algorithm (SSA). Lu et al. [18] propose a novel handwriting-based PD detection method by extracting kinematic, pressure, and angle dynamic features and optimizing classification performance utilizing the escape Coati Optimization Algorithm (eCOA). Majhi et al. [19] propose four DL models with a hybrid approach for early PD detection, utilizing Grey Wolf Optimization (GWO) for fine-tuning. Jain and Srivastava [20] present an FLSNN framework to enhance the detection of neurological disorders from EEG signals by utilizing fuzzy logic to handle uncertainties and spiking neural networks for dynamic signal analysis. Hadadi and Arabani [21] introduce a DL-based disease diagnosis method utilizing handwritten samples optimized with the Harris Hawks Optimization (HHO) technique for improved performance.

Mallidi and Ramisetty [22] introduce Bowerbird Courtship-Inspired Feature Selection (BBFS), a meta-heuristic methodology that optimizes feature selection by balancing exploration and exploitation. Cuk et al. [23] use Long Short-Term Memory (LSTM) with attention mechanisms to detect PD from dual-task walking data, proposing a modified Crayfish Optimization Algorithm (COA) model to improve the performance of the model. Ekinici et al. [24] utilize the Sinh Cosh Optimizer (SCHO) technique, enhancing tuning by overcoming local minima and exhibiting convergence issues in conventional methods. Cincovic et al. [25] integrate Artificial Intelligence (AI) and ML techniques for early PD from finger-tapping accelerometer data, using RNNs, and extreme gradient boosting. Metaheuristics, comprising a modified Sinh cosh optimizer, are employed to optimize performance. KV and Selvakumar [26] present a Personalized Recommendation System for Early-Stage Skin Cancer Detection (PRSSCHM) approach using a hybrid model. It comprises preprocessing, deep joint segmentation, feature extraction (MBP, GLCM, ILDTP), and Improved Bi-LSTM and DBN classification. The IBEASO method optimizes model weights for accurate classification. Sawan et al. [27] propose a hybrid DL method combining CNN and BiGRU for stroke classification from EEG data, optimized with Harmony Search (HS) and Multiverse Optimization (MVO)-based extraction and tuning. Despite improvements in PD detection using various approaches such as CSSFOA, ACSA, ISFO-DL, etc., challenges remain in optimizing performance across diverse datasets and ensuring real-time applicability. Many models

face difficulty with overfitting, computational complexity, and limited generalizability across various populations. Additionally, there is a requirement for better integration of hybrid models (e.g., DL + metaheuristics) for enhanced accuracy and efficiency in real-world applications. Future research may optimise hybrid models and reduce the computational burden for practical deployment.

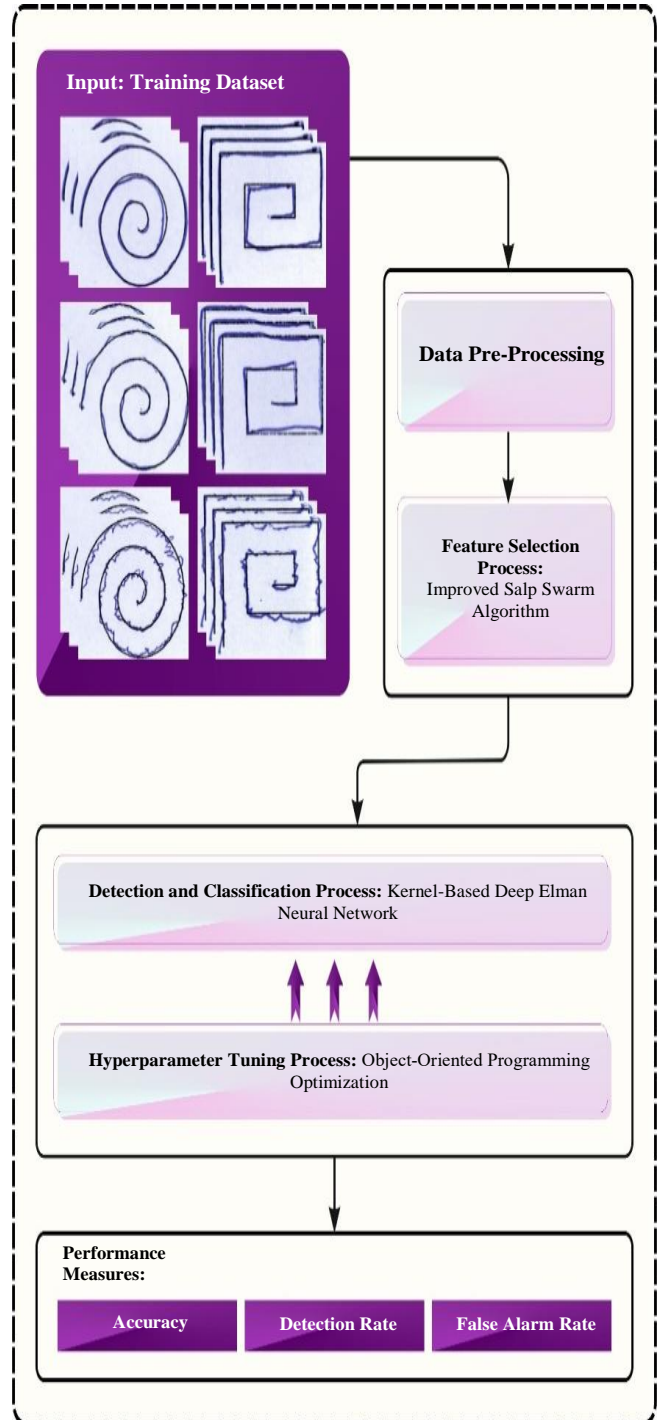


Fig. 1 Workflow of HMDL-PDDC technique

### 3. The Proposed Methodology

In this paper, a new HMDL-PDDC technique is proposed. The method follows the design of a hybrid metaheuristics-based FS with an optimum DL technique for recognizing and identifying PD. To accomplish that, the HMDL-PDDC technique involves three main sub-processes: ISSA-based feature subset selection, KDENN-based classification, and OPOA-based tuning. Figure 1 illustrates the flow of the HMDL-PDDC model.

#### 3.1. FS Using ISSA

Initially, the HMDL-PDDC technique undergoes the selection of feature subsets using ISSA. Salps are sea invertebrates that look identical to jellyfish and show swarm behaviour when looking for prey, which is recognized as a salp chain [28]. The SSA has prominent benefits like fast convergence to the optimum value and the least desire to alter its limits. These effects create this meta-heuristic process appropriate for a swarm of optimizer issues exact to engineering areas like power systems. SSA is used to proficiently allocate single-phase load among three phases of a distribution system, whereas the authors present an SSA-based technique for Maximum Power Point Tracking (MPPT). SSA can attain the optimum transient response through dissimilar operating conditions. In a salp chain populace, there is a cluster and elected leader. The leader is highly in charge of searching, while the groups energetically alter their locations and so in closeness to the leader. At every iteration  $p$ , the leader location in the salp-chain  $X_1^{(p)}$  has been upgraded by the position of the food source  $F^{(p)}$  utilizing the formula:

$$X_1^{(p)} = \begin{cases} F^{(p)} + c_1((X_{\max} - X_{\min})c_2 + X_{\min}), & c_3 > 0.5 \\ F^{(p)} - c_1((X_{\max} - X_{\min})c_2 + X_{\min}), & c_3 \leq 0.5 \end{cases} \quad (1)$$

Where  $X_{\max}$  and  $X_{\min}$  represent the lower and upper limits,  $C3$  and  $C2$  are randomly produced in  $[0,1]$ . To calculate parameter  $C1$ , the following formula has been used:

$$c_1 = 2e^{-\left(\frac{4t}{t_{MAX}}\right)^2} \quad (2)$$

Whereas  $t$  signifies the present iteration step,  $t_{MAX}$  denotes the total iteration count measured.

As the location of a leader is upgraded, every follower alters its place  $X_k^{(p)}$  dependent on the preceding salp in the chain  $X_{k-1}^{(p)}$ :

$$X_k^{(p)} = \frac{1}{2}(X_k^{(p)} + X_{k-1}^{(p)}) \quad (3)$$

The conventional SSA presents many benefits, such as a chance for alterations to improve convergence rapidity while upholding stability amid the exploitation and exploration

stages. So, many enhanced types of SSA were developed in the study. A hybrid among an SSA and SCA has been presented, whereas the author projects an operator of sine cosine and Levy flight to enhance the performance of the SSA. A chaotic map is given to enhance the performance of SSAs and suggests an operator of mutation to improve the SSA's search abilities. The preceding work is extended for the ISSO by developing two novel social classes: Rogue Salp (RS) and Pioneer Salp (PS).

The PS improves the search phase by operating independently of the Leader Salp. For this reason, every PS will arbitrarily select an equivalent possibility. In the first case, the PS location is defined by including a random difference to a salp  $X$  and described in Equation (4). The second PS location upgrade device contains a random linear mixture among two nominated salps  $X_{R,1}$  and  $X_{R,2}$ . In contrast, the third choice embodies producing a novel random location, as defined in Equation (5) and (6). The fourth substitute for determining the PS location depends on the opposition-based learning standard. Therefore, the present location of the PS is defined as opposed to its preceding location, as assumed in Equation (7). It must be stated that  $r1$  and  $r2$  from Equation (4)-(7) are random facts within the interval  $[0,1]$ , whereas  $X_{\min}$  and  $X_{\max}$  represent the lower and upper bounds.

$$X_k^{(p)} = X_R^{(p-1)} + r_1 \cdot [r_2 \cdot (X_{\max} - X_{\min}) + X_{\min}] \quad (4)$$

$$x_k^{(p)} = r_1 \cdot X_{R,1}^{(p-1)} + (1 - r_1) \cdot x_{R,2}^{(p-1)} \quad (5)$$

$$X_k^{(p)} = r_1 \cdot (X_{\max} - X_{\min}) + X_{\min} \quad (6)$$

$$X_k^{(p)} = X_{\max} + X_{\min} - X_k^{(p-1)} \quad (7)$$

The RS is proposed to expand the performance of ISSAs in the exploitation stage. The RS also travel near the prey, but they refuse to obey Leader Salp's rules and define their future location, relying on their real location and food source.

$$x_k^{(p)} = F_k^{(p-1)} + r_1 \cdot [r_2 \cdot F_k^{(p-1)} - (1 - r_2) \cdot x_k^{(p-1)}] \quad (8)$$

$r1$  and  $r2$  denote a random amount within the range of  $[-0.5,0.5]$  and  $[0,1]$ , respectively. The  $[-0.5,0.5]$  interval is selected for the  $r1$  values to guarantee discrepancies in both increase ( $r1 > 0$ ) and decrease ( $r1 < 0$ ) the values of the salp location.

The traditional SSA location upgrade device for the Follower Salps, assumed in Equation (3), has been adapted in enhanced form by producing a random linear mixture among the binary successive salps.

$$x_k^{(p)} = r_1 \cdot x_{k-1}^{(p-1)} + (1 - r_1) \cdot x_k^{(p-1)} \quad (9)$$

For every salp, excluding the leader, an arbitrary amount  $r \in [0,1]$  is produced. At first, there is a  $pfoll$ , or possibility of becoming a Follower Salp (if  $r < pfoll$ ). If the existing salp is not a follower, then a novel number of random  $r \in [0,1]$  has been produced. The  $ppion$  possibility of being a PS (if  $r < ppion$ ) or (if  $r \geq ppion$ ), it will become an RS. The probability  $pfoll$  rises linearly from  $p_{foll}^{min}$  to  $p_{foll}^{max}$  throughout the iterations, whereas the  $ppion$  probability reduces linearly from  $p_{pion}^{max}$  to  $p_{pion}^{min}$  as iterations grow:

$$p_{foll} = \frac{p}{p_{max}} \cdot (p_{foll}^{max} - p_{foll}^{min}) + p_{pion}^{min} \quad (10)$$

$$p_{pion} = \left(1 - \frac{p}{p_{max}}\right) \cdot (p_{pion}^{max} - p_{pion}^{min}) + p_{pion}^{min} \quad (11)$$

The ISSA model integrates the objectives into a single unified formulation, where each current weight defines the importance of every objective [29]. In this study, an FF is used, which incorporates both FS as presented in (12).

$$Fitness(X) = \alpha \cdot E(X) + \beta \cdot \left(1 - \frac{|R|}{|N|}\right) \quad (12)$$

Here,  $Fitness(X)$  depicts the fitness value of a subset  $X$ ;  $|R|$  and  $|N|$  is the number of nominated and original features, correspondingly;  $E(X)$  depicts the classification error rate by employing the chosen features in the  $X$  subset;  $\beta$  and  $\alpha$  denotes the reduction ratio weight and classification error,  $\beta = (1 - \alpha)$  and  $\alpha \in [0,1]$ .

### 3.2. DENN-Based Classification

In this work, the KDENN technique is exploited to detect and classify PD. As a partial recurrent network model, the classical ENN includes the context, HL, and input and output layers [30].

The deviation between the feedforward neural network and ENN is the presence of a context layer that memorizes the HL's output as an operator of step delay.

The presented model intensely studies the data by clarifying the data through the  $n$ -number of HLs to decrease the training error higher than the  $n$ -amount of HLs.

This DL technique provides an accurate classification. The feature extracted is fed into the KDENN classifier. Figure 2 shows the KDENN framework.

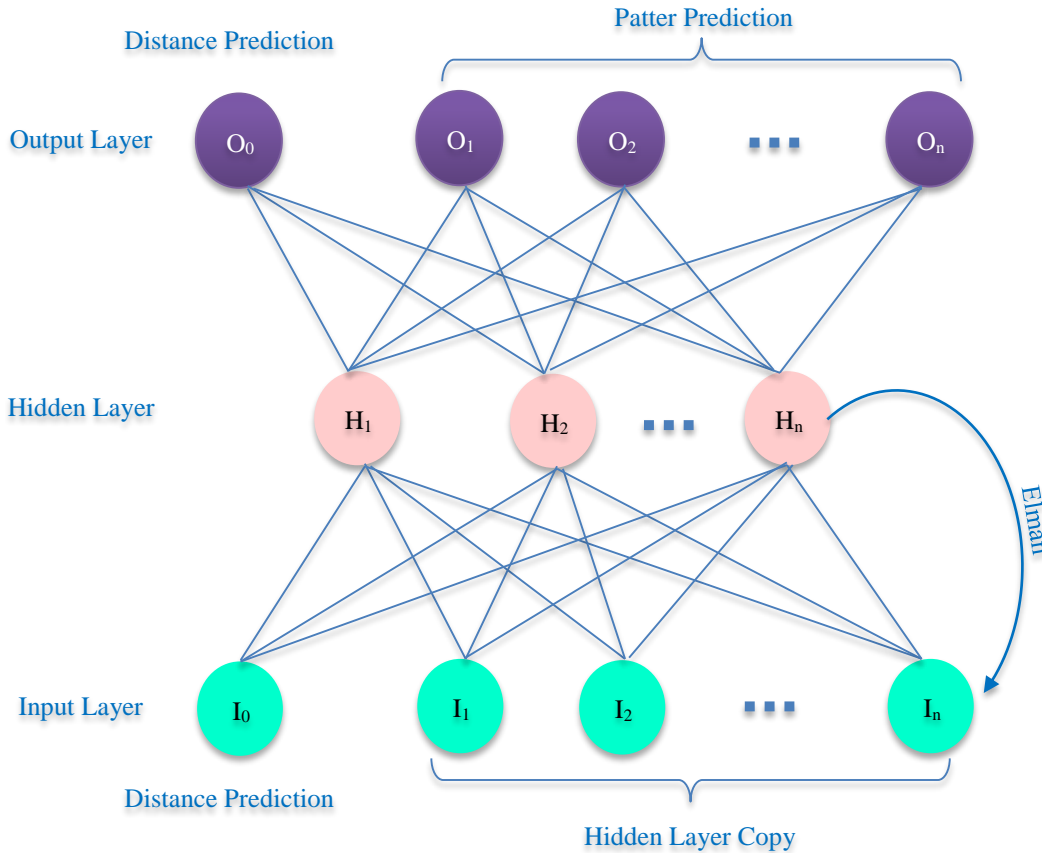


Fig. 2 Architecture of KDENN

The input layer has  $N$ -dimension external input vector  $Z_{f,N}$ . The weight value for the inputted feature value is arbitrarily produced. Then, these values are transmitted to the HL as follows:

$$O_{HID,\tilde{t}} = \kappa_H \left( W_{IH} O_{CON,\tilde{t}} + W_{HC} (Z_{f,N}) \right) \quad (13)$$

In Equation (13),  $O_{HID,\tilde{t}}$  shows the output HLs at  $\tilde{t}$  iteration;  $O_{HID,\tilde{t}}$  indicates the output HL unit at  $\tilde{t}$  iteration;  $O_{CON,\tilde{t}}$  refers to the output context layer unit at  $\tilde{t}$  iteration, correspondingly. The output context layer is represented as follows:

$$O_{CON,\tilde{t}} = O_{HIDD,\tilde{t}-1} \quad (14)$$

In Equation (14),  $W_{IH}$  implies the weight of the input layer to HL;  $O_{HIDD,\tilde{t}-1}$  signifies the output HLs at  $\tilde{t} - 1$  iteration;  $\kappa_H$  implies the kernel activation function;  $W_{HC}$  symbolizes the weight of HL. Rather than the Gaussian activation function,  $\kappa_H$  is applied in the KDENN.  $\kappa_H$  has a robust performance in the DL-NN model. The  $\kappa_H$  is expressed as

$$\kappa(\alpha) = \sum_N \beta_N k(\alpha, d_N) \quad (15)$$

In Equation (15),  $\kappa(\alpha)$  implies the  $\kappa_H$  aimed at input  $\alpha$ ;  $\beta_N$  signifies the mixed coefficients;  $d_N$  denotes the dictionary element;  $k$  indicates the kernel coefficient. Before  $\kappa_H$ , the HL provides output  $O_{HID,\tilde{t}}$  as input to the output layer. Gr on output HLs, the output layer produces the final output as follows:

$$O_{OUT,\tilde{t}} = \kappa_O (W_{HO} O_{HID,\tilde{t}}) \quad (16)$$

In Equation (16),  $O_{OUT,\tilde{t}}$  shows the output layer unit;  $\kappa_O$  depicts the activation function of the output layer;  $W_{HO}$  suggests the weight of HL to the output layer.

### 3.3. Hyperparameter Tuning by Utilizing the OOPOA

Finally, OOPOA executes the selection of the KDENN hyperparameter technique. OOPOA is a new meta-heuristic that imitates the instructions through which features are exchanged among objects of various classes in OOP [31]. These instructions have been called access modifiers that find where the class elements will be retrieved. In an OOPOA, the outcomes of the early populace signify diverse classes in the application, and the elements describe the feature to be transferred amongst classes. Such features have been exchanged based on the access modifier instructions. Distribution features among solutions can offer the production of an upgraded population. Subsequently, the population could be improved repetitively up to the maximum number of iterations that will be gained. The phases of OOPOA are given below: Initially, 2 vectors must be arbitrarily initialized. The 1<sup>st</sup> vector signifies the initial population  $X$  is given

$$X = \begin{bmatrix} X_{1,1} & X_{1,2} & X_{1,D-1} & X_{1,D} \\ X_{2,1} & X_{2,2} & X_{2,D-1} & X_{2,D} \\ \vdots & \vdots & \vdots & \vdots \\ X_{N-l,1} & X_{N-l,2} & X_{N-l,D-1} & X_{N-l,D} \\ X_{N,1} & X_{N,2} & X_{N,D-1} & X_{N,D} \end{bmatrix} \quad (17)$$

The 2<sup>nd</sup> vector will be named the status vector  $S$ , with a similar dimension as the populace vector as expressed below:

$$S = \begin{bmatrix} S_{1,1} & S_{1,2} & S_{1,D-1} & S_{1,D} \\ S_{2,1} & S_{2,2} & S_{2,D-1} & S_{2,D} \\ \vdots & \vdots & \vdots & \vdots \\ S_{N-l,1} & S_{N-l,2} & S_{N-l,D-1} & S_{N-l,D} \\ S_{N,1} & S_{N,2} & S_{N,D-1} & S_{N,D} \end{bmatrix} \quad (18)$$

$S_{ii}$  represents the prominence of the feature.  $S_{ii}$  refers to a value from 0, 1 and 2 that denotes three common access modifiers: protected, public, and private.

1. To upgrade the population, a parent decision (solution with maximum fitness) was chosen for exchanging its features with alternative solutions at a population as stated in the value of its features as given:
  - The variable resultant position value is *zero*, a public variable that describes every solution at population can get variable:

$$X_{k_i l} = \begin{cases} P_l & \text{if } S_l = 0 \\ X_{k,l} & \text{if } S_l = 1 \\ X_{k,l} & \text{if } S_l = 2 \end{cases} \quad (19)$$

Whereas  $P_1$  is the lh component in the parent  $P$ ,  $S_1$  is the  $l$ -th constituent in the status vector for the parent  $P$ ,  $X_{k,l}$  signifies the  $l$ -th element in the  $k^{th}$  solution. The values of 0,1 and 2 correspondingly describe private, public, and protected status.

- A child solution has been randomly set and assumes each protected and public feature in the parent solution given below:

$$Ch_l = \begin{cases} P_l & \text{if } S_l = 0, \\ P_l & \text{if } S_l = 1 \\ \text{rand}(lb, ub) & \text{otherwise.} \end{cases} \quad (20)$$

Here,  $lb$  and  $ub$  depict the lower and upper limits and  $Ch_l$  represents the  $lh$  component in the child  $Ch$ .

- Once the newly generated child is more suitable than the parent, it replaces the parent; otherwise, the parent is retained for the next generation.
2. A mutation procedure must be implemented to the position vector to upsurge the variety of decisions and prevent the problem of getting stuck at local minima, s:

$$S_j(u) = \begin{cases} \text{rfrand}(0, 1) < MR \\ S_{u \text{ otherwise}} \end{cases} \quad (21)$$

Where  $S_i(u)$  denotes the variable in position  $u$  in the vector  $S_i$ ,  $um = 1, 2, \dots, D$ ;  $S_i$  refers to the status vector of the

$i^{th}$  the solution,  $i = 1, 2, \dots, N$  and MR refers to the mutation rate, obtaining a value in the interval  $[0.1, 0.99]$ . The OPOA method, derived from an FF, improves classification performance by defining an optimistic value to represent the optimal candidate output. In this study, the error minimization rate of the classifier is treated as the FF, as shown in Equation (22).

$$fitness(x_i) = \frac{ClassifierErrorRate(x_i) \times 100}{Total\ no.\ of\ samples} \quad (22)$$

#### 4. Result Analysis

In this part, the simulation values of the HMDL-PDDC model are accomplished by utilizing four datasets, namely

HandPD Spiral (HandPDS), HandPD Meander (HandPDM), Voice PD (VPD) datasets and Speech PD (SPD).

The technique is simulated by utilizing the Python 3.6.5 tool on PC i5-8600k, 250GB SSD, GeForce 1050Ti 4GB, 16GB RAM, and 1TB HDD. The parameter settings are provided in the following: learning rate: 0.01, activation: ReLU, epoch count: 50, dropout: 0.5, and batch size: 5.

Table 1 and Figure 3 signify the FS outcomes of the HMDL-PDDC method on four datasets. The outcomes implied that the HMDL-PDDC technique selected a minimum feature number equated to other approaches. It is noticeable that the HMDL-PDDC method has nominated 5, 8, 11, and 8 features below the four datasets, correspondingly.

Table 1. FS analysis of the HMDL-PDDC technique on four datasets

| Dataset  | Overall Features | MGOA | MGWO | OCFA | IFSO-DL | ISSA-FS |
|----------|------------------|------|------|------|---------|---------|
| Hand PDS | 13               | 5    | 7    | 8    | 4       | 3       |
| Hand PDM | 13               | 8    | 8    | 7    | 6       | 5       |
| SPD      | 23               | 11   | 12   | 13   | 10      | 6       |
| VPD      | 26               | 8    | 9    | 17   | 7       | 5       |

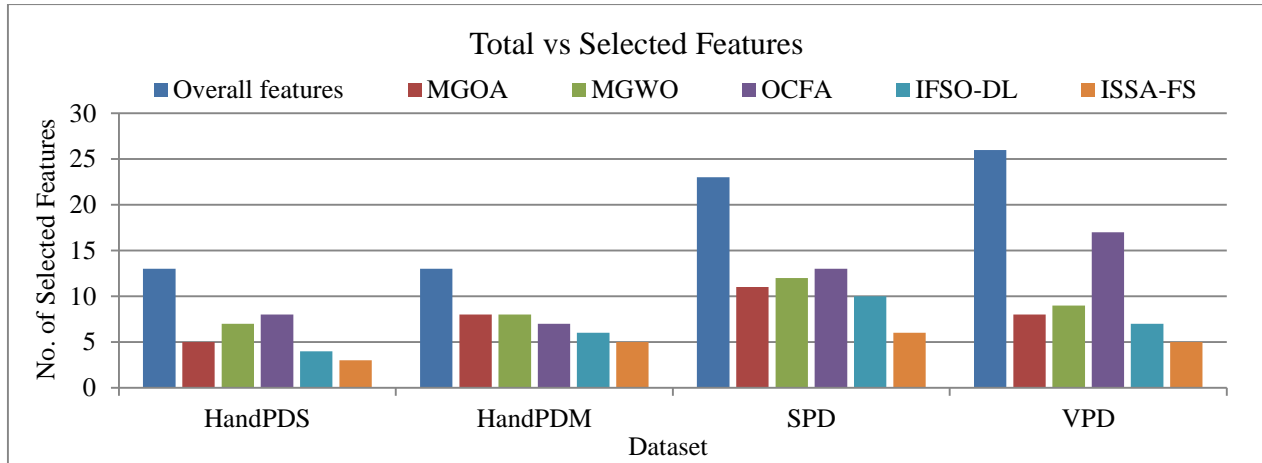


Fig. 3 FS analysis of HMDL-PDDC technique on four datasets

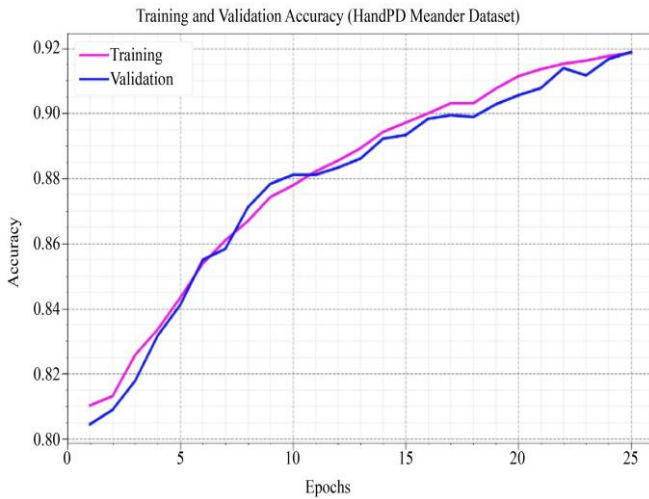
Table 2. Comparative analysis of the HMDL-PDDC method on the HandPDM dataset

| HandPDM Dataset |          |             |       |
|-----------------|----------|-------------|-------|
| Methods         | Accuracy | DR (Recall) | FAR   |
| MGOA-KNN        | 74.80    | 85.80       | 47.60 |
| MGOA-RF         | 93.70    | 97.89       | 19.10 |
| MGOA-DT         | 89.00    | 91.80       | 16.70 |
| MGWO-KNN        | 72.80    | 85.80       | 60.00 |
| MGWO-RF         | 93.00    | 98.10       | 22.20 |
| MGWO-DT         | 88.00    | 92.00       | 22.20 |
| IFSO-DL         | 94.00    | 95.23       | 13.50 |
| HMDL-PDDC       | 94.97    | 98.31       | 08.87 |

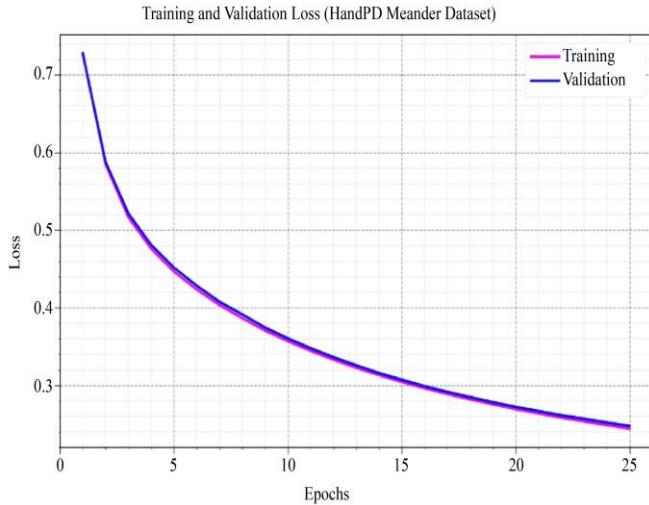
Table 2 highlights the comparative results of the HMDL-PDDC technique on the HandPDM dataset [13]. The outputs imply that the MGOA-KNN and MGWO-KNN methods have portrayed the least results. Followed by the MGOA-DT and MGWO-DT models have managed to reach closer results. Likewise, the MGOA-RF, MGWO-RF, and IFSO-DL models attained reasonable performance. Finally, the HMDL-PDDC method gains maximum performance with  $accu_y$  of 94.97%, Detection Rate (DR) of 98.31%, and FAR of 8.87%.

Figure 4 depicts the Training Accuracy (TRAA) and Validation Accuracy (VALA) curves of the HMDL-PDDC method. The figure provides insights into the model's behaviour over various epochs, emphasizing its learning and

generalization abilities. The results show significant improvement as the epochs grow, confirming the adaptability of the HMDL-PDDC approach in detecting patterns in both TRA/TES data. The rise in VALA indicates the model's capability to generalize well, effectively identifying unseen data. Figure 5 illustrates the Training Loss (TRLA) and Validation Loss (VALL) of the HMDL-PDDC approach on the HandPDM dataset across diverse epochs. The decrease in TRLA shows that the HMDL-PDDC method effectually optimizes weights and reduces classification errors in TRA/TES data. The figure highlights its capability to identify patterns in both datasets while refining parameters to minimize discrepancies between predicted and actual TRA classes.



**Fig. 4** *Accu*, the curve of the HMDL-PDDC method on the Handpdm dataset



**Fig. 5** Loss curve of HMDL-PDDC method on HandPDM dataset

Table 3 highlights the comparison outputs of the HMDL-PDDC method on the HandPDS dataset. The results show that the HMDL-PDDC technique outperforms others with an

*accu<sub>y</sub>* of 93.98%, DR of 98.57%, and FAR of 6.61%, achieving the highest performance compared to alternative methods, whereas other models exhibited lesser performance.

**Table 3.** Comparative evaluation of the HMDL-PDDC method on the HandPDS dataset

| HandPDS Dataset |          |             |       |
|-----------------|----------|-------------|-------|
| Methodologies   | Accuracy | DR (Recall) | FAR   |
| MGOA-KNN        | 75.60    | 85.30       | 53.10 |
| MGOA-RF         | 92.90    | 97.90       | 21.90 |
| MGOA-DT         | 89.00    | 94.70       | 28.10 |
| MGWO-KNN        | 73.40    | 81.90       | 50.00 |
| MGWO-RF         | 92.40    | 94.00       | 11.90 |
| MGWO-DT         | 92.40    | 94.00       | 11.90 |
| IFSO-DL         | 93.30    | 98.20       | 8.00  |
| HMDL-PDDC       | 93.98    | 98.57       | 6.61  |

The accomplishment of the HMDL-PDDC technique on the HandPDS dataset is shown in Figure 6 through the TRAA/VALA curves. The figure illustrates the performance of the HMDL-PDDC approach across epochs, showing a steady increase in both TRAA and VALA.

This underscores the capability of the method to adapt and generalize, effectually detect patterns in both TRA and TES data, and demonstrate robust performance on unseen data.

Figure 7 represents the TRLA/VALL results of the HMDL-PDDC approach on the HandPDS dataset over separate epochs. The decrease in TRLA demonstrates the HMDL-PDDC approach, optimizing weights and mitigating TRA/TES data classification errors. The figure emphasizes the capability of the model to capture patterns in both datasets, improving parameters and minimizing discrepancies between anticipated and actual TRA classes.

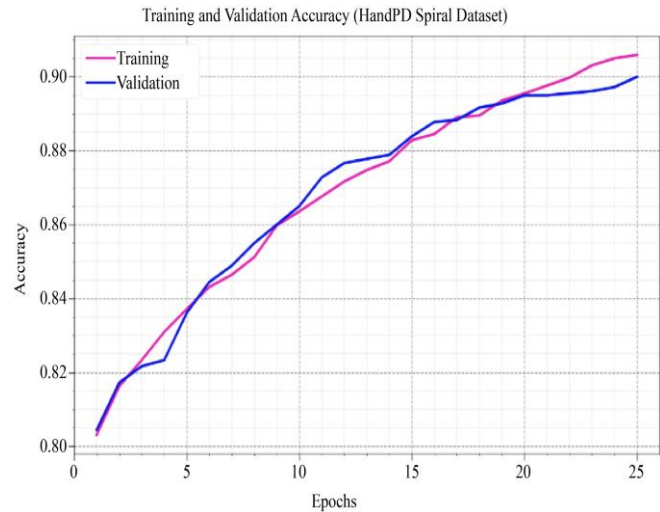


**Fig. 6** *Accu*, the curve of the HMDL-PDDC method on the HandPDS dataset

Table 4 highlights the comparative outputs of the HMDL-PDDC technique on the SPD dataset. The HMDL-PDDC methodology demonstrated the greatest output with  $accu_y$  of 97.10%, DR of 98.73%, and FAR of 10.00%, whereas other techniques illustrated lesser outputs.

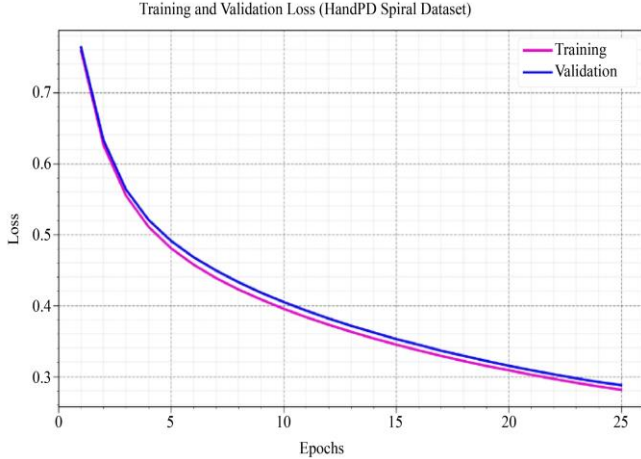


Fig. 7 Loss curve of HMDL-PDDC method on HandPDS dataset

Table 4. Comparative analysis of HMDL-PDDC technique on SPD dataset

| SPD Dataset |          |             |       |
|-------------|----------|-------------|-------|
| Methods     | Accuracy | DR (Recall) | FAR   |
| MGOA-KNN    | 89.70    | 96.70       | 30.00 |
| MGOA-RF     | 94.90    | 97.67       | 22.20 |
| MGOA-DT     | 84.60    | 90.00       | 30.00 |
| MGWO-KNN    | 91.80    | 97.40       | 30.00 |
| MGWO-RF     | 93.90    | 98.56       | 30.00 |
| MGWO-DT     | 89.80    | 94.90       | 30.00 |
| IFSO-DL     | 95.30    | 96.32       | 18.50 |
| HMDL-PDDC   | 97.10    | 98.73       | 10.00 |

Figure 9 provides the TRLA/VALL results of the HMDL-PDDC method on the SPD dataset across diverse epochs. The mitigation in TRLA shows the capability of the HMDL-PDDC method to refine weights and minimize classification errors on both TRA/TES data. The figure depicts the HMDL-PDDC alignment of the model with the TRA data, showing its capability to comprehend patterns in both datasets. The HMDL-PDDC technique steadily grows its parameters to mitigate the discrepancies between anticipated and actual TRA classes.

The performance of the HMDL-PDDC methodology on the SPD dataset is depicted in Figure 8 through the TRAA/VALA curves. The figure highlights the HMDL-PDDC methodology's learning and generalization across epochs, showing consistent improvement in TRAA/VALA. It emphasizes the model's adaptive behavior in detecting patterns in TRA/TES data and its ability to accurately classify unseen data, depicting robust generalization capabilities.

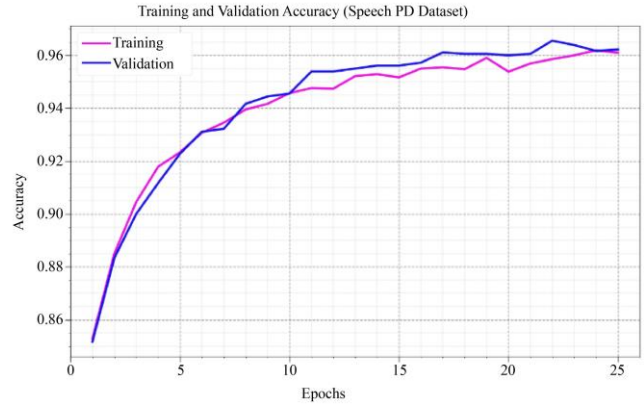
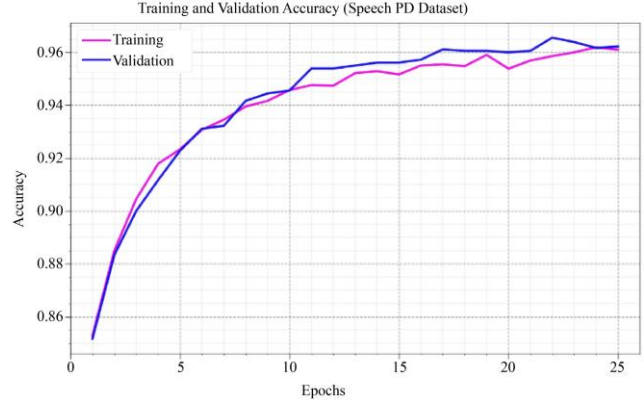


Fig. 8  $Accu_y$  curve of the HMDL-PDDC method on the SPD dataset

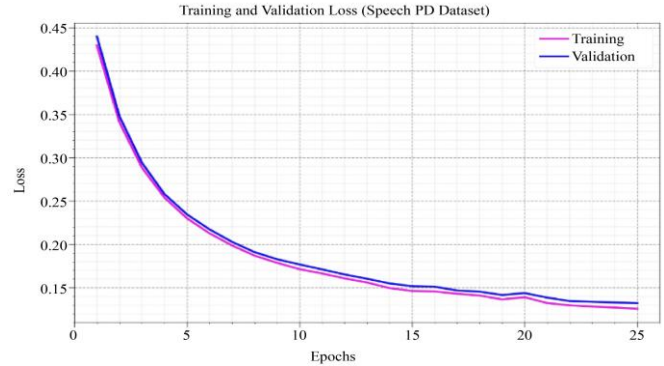


Fig. 9 Loss curve of HMDL-PDDC method on SPD dataset

Table 5. Comparative analysis of the HMDL-PDDC technique on the VPD dataset

| VPD Dataset   |          |             |       |
|---------------|----------|-------------|-------|
| Methodologies | Accuracy | DR (Recall) | FAR   |
| MGOA-KNN      | 91.80    | 83.50       | 43.90 |
| MGOA-RF       | 95.70    | 95.40       | 32.00 |
| MGOA-DT       | 96.23    | 95.78       | 41.00 |
| MGWO-KNN      | 85.80    | 80.30       | 28.10 |
| MGWO-RF       | 95.89    | 96.39       | 21.50 |
| MGWO-DT       | 97.01    | 98.14       | 28.19 |
| IFSO-DL       | 98.24    | 97.80       | 17.31 |
| HMDL-PDDC     | 98.71    | 98.59       | 09.08 |

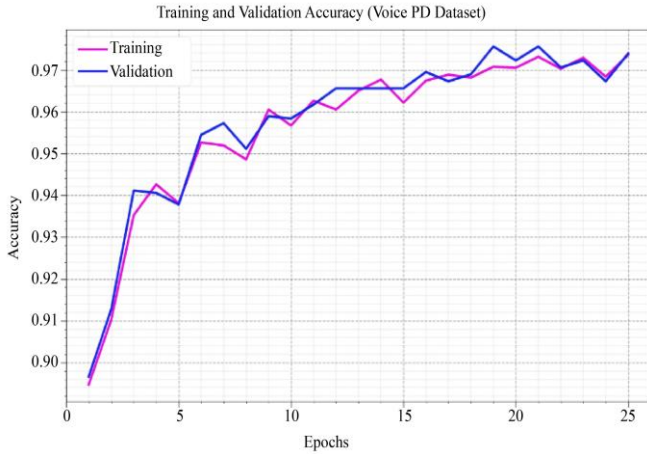


Fig. 10 *Accu<sub>y</sub>* curve of the HMDL-PDDC method on the VPD dataset

Table 5 highlights the comparison outputs of the HMDL-PDDC method on the VPD dataset. The HMDL-PDDC method attained the greatest performance with *accu<sub>y</sub>* of 98.71%, DR of 98.59%, and FAR of 09.08%, whereas other methodologies exhibited lesser outcomes. The accomplishment of the HMDL-PDDC approach on the VPD dataset is shown in Figure 10 through the TRAA/VALA curves. The figure shows the progress of the HMDL-PDDC approach across epochs, with consistent improvements in TRAA and VALA.

This accentuates its adaptability in detecting patterns in both TRA and TES data, illustrating robust generalization and accurate classification of unseen data. Figure 11 provides the TRLA/VALL results for the HMDL-PDDC technique on the VPD dataset across various epochs. The lessening in TRLA shows the efficiency of the HMDL-PDDC approach in optimizing weights and minimizing classification errors for both TRA/TES data. The figure clearly comprehends the

HMDL-PDDC model's alignment with the TRA data, showing its capability to capture patterns in both datasets. Notably, the HMDL-PDDC technique consistently refines its parameters, mitigating the discrepancies between anticipated and actual TRA classes. Figure 12 illustrates a complete comparative study of the HMDL-PDDC model with recent techniques on four datasets regarding *accu<sub>y</sub>*. Experimentation showed that the HMDL-PDDC method outperformed existing approaches with the highest *accu<sub>y</sub>* values under every database. Figure 13 determines a general comparison evaluation of the HMDL-PDDC approach with existing methods on four datasets regarding DR. The experimental outcomes indicate that the HMDL-PDDC method outperformed existing techniques with the highest DR values in every dataset. Figure 14 shows the comparison evaluation of the HMDL-PDDC approach with existing techniques on four databases regarding FAR. The outputs clearly show that the HMDL-PDDC method outperformed existing techniques, with the least FAR values below each dataset. These results showcase the effective ability of the HMDL-PDDC technique in the PD recognition process.

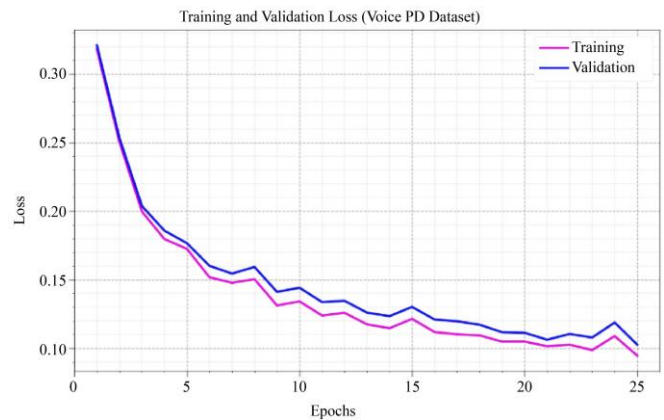


Fig. 11 Loss curve of HMDL-PDDC method on VPD dataset

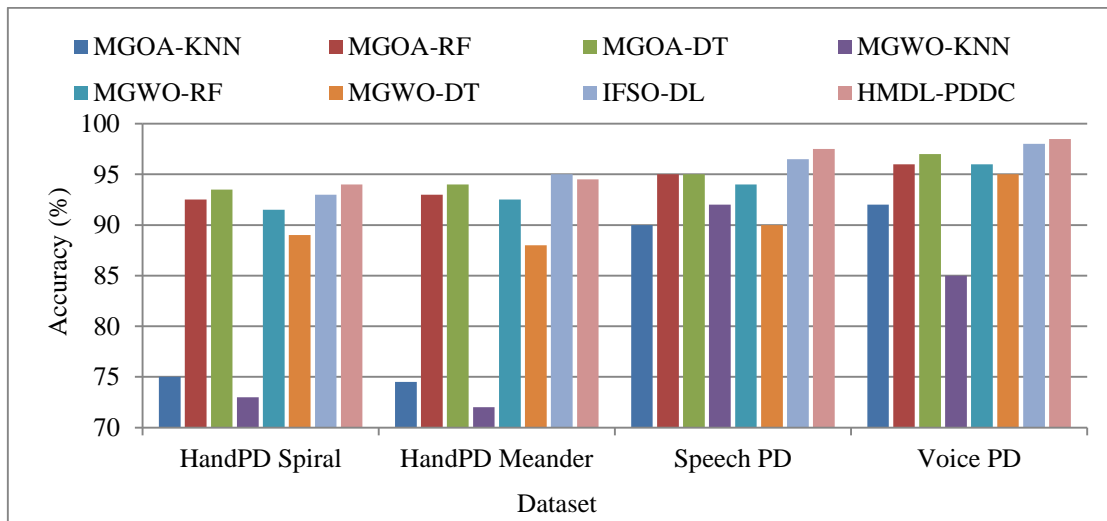


Fig. 12 *Accu<sub>y</sub>* analysis of the HMDL-PDDC technique under four datasets

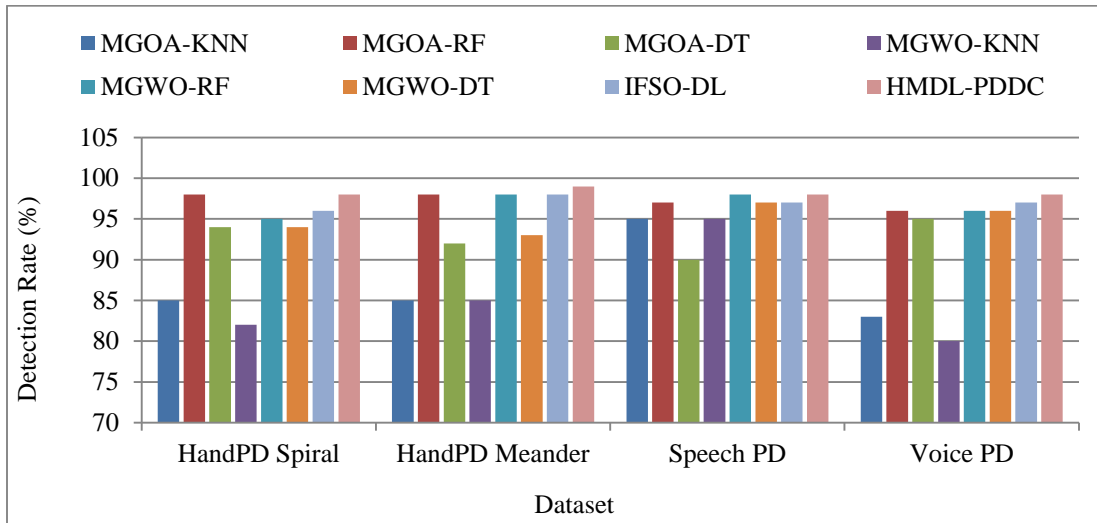


Fig. 13 DR analysis of the HMDL-PDDC technique under four datasets

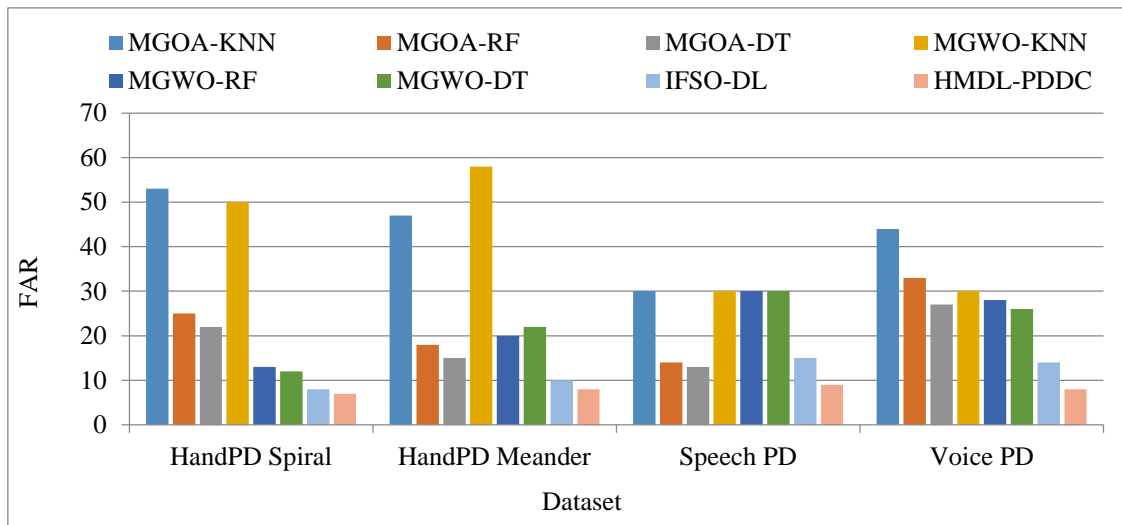


Fig. 14 FAR analysis of HMDL-PDDC technique under four datasets

## 5. Conclusion

In this paper, an innovative HMDL-PDDC approach is presented. The HMDL-PDDC approach follows the design of hybrid metaheuristics-based FS with an optimum DL technique for recognizing and identifying PD. To accomplish that, the HMDL-PDDC approaches contain three main sub-processes: ISSA-based feature subset selection, KDENN-based classification, and OPOA-based tuning. Primarily, the

HMDL-PDDC technique is used to select feature subsets using ISSA. Besides, the KDENN model is exploited to recognize and identify PD. Moreover, OPOA selects the hyperparameter of the KDENN model. The experimentation outcomes of the HMDL-PDDC model are examined under four datasets using a set of measures. The experimental validation of the HMDL-PDDC technique portrayed superior accuracy values of 93.98%, 94.97%, 98.71% and 97.10% over existing models.

## References

- [1] Amin Ul Haq et al., "Feature Selection Based on L1-Norm Support Vector Machine and Effective Recognition System for Parkinson's Disease Using Voice Recordings," *IEEE Access*, vol. 7, pp. 37718-37734, 2019. [CrossRef] [Google Scholar] [Publisher Link]
- [2] Ozkan Cigdem, and Hasan Demirel, "Performance Analysis of Different Classification Algorithms Using Different Feature Selection Methods on Parkinson's Disease Detection," *Journal of Neuroscience Methods*, vol. 309, pp. 81-90, 2018. [CrossRef] [Google Scholar] [Publisher Link]

- [3] Gunjan Pahuja, and T. N. Nagabhusan, "A Comparative Study of Existing Machine Learning Approaches for Parkinson's Disease Detection," *IETE Journal of Research*, vol. 67, no. 1, pp. 4-14, 2018. [[CrossRef](#)] [[Google Scholar](#)] [[Publisher Link](#)]
- [4] Liaqat Ali et al., "Early Diagnosis of Parkinson's Disease from Multiple Voice Recordings by Simultaneous Sample and Feature Selection," *Expert Systems with Applications*, vol. 137, pp. 22-28, 2019. [[CrossRef](#)] [[Google Scholar](#)] [[Publisher Link](#)]
- [5] Amira S. Ashour et al., "A Novel Framework of Two Successive Feature Selection Levels Using Weight-Based Procedure for Voice-Loss Detection in Parkinson's Disease," *IEEE Access*, vol. 8, pp. 76193-76203, 2020. [[CrossRef](#)] [[Google Scholar](#)] [[Publisher Link](#)]
- [6] Gabriel Solana-Lavalle, and Roberto Rosas-Romero, "Classification of PPMI MRI Scans with Voxel-based Morphometry and Machine Learning to Assist in the Diagnosis of Parkinson's Disease," *Computer Methods and Programs in Biomedicine*, vol. 198, pp. 1-15, 2021. [[CrossRef](#)] [[Google Scholar](#)] [[Publisher Link](#)]
- [7] Rohit Lamba, Tarun Gulati, and Anurag Jain, "Comparative Analysis of Parkinson's Disease Diagnosis System," *Advances in Mathematics: Scientific Journal*, vol. 9, no. 6, pp. 3399-3406, 2020. [[CrossRef](#)] [[Google Scholar](#)] [[Publisher Link](#)]
- [8] C. Okan Sakar et al., "A Comparative Analysis of Speech Signal Processing Algorithms for Parkinson's Disease Classification and the Use of the tunable Q-Factor Wavelet Transform," *Applied Soft Computing*, vol. 74, pp.255-263, 2019. [[CrossRef](#)] [[Google Scholar](#)] [[Publisher Link](#)]
- [9] Iqra Nissa et al., "Voice-Based Detection of Parkinson's Disease through Ensemble Machine Learning Approach: A Performance Study," *EAI Endorsed Transactions on Pervasive Health and Technology*, vol. 5, no. 19, pp. 1-8, 2019. [[CrossRef](#)] [[Google Scholar](#)] [[Publisher Link](#)]
- [10] Rohit Lamba et al., "A Hybrid System for Parkinson's Disease Diagnosis using Machine Learning Techniques," *International Journal of Speech Technology*, vol. 25, pp. 583-893, 2021. [[CrossRef](#)] [[Google Scholar](#)] [[Publisher Link](#)]
- [11] M.K. Dharani, and R.B. Thamilselvan, "Hybrid Optimization Enabled Deep Learning Model for Parkinson's Disease Classification," *The Imaging Science Journal*, vol. 72, no. 2, pp. 167-182, 2024. [[CrossRef](#)] [[Google Scholar](#)] [[Publisher Link](#)]
- [12] Mehedi Masud et al., "CROWD: Crow Search and Deep Learning based Feature Extractor for Classification of Parkinson's Disease," *ACM Transactions on Internet Technology*, vol. 21, no. 3, pp. 1-18, 2021. [[CrossRef](#)] [[Google Scholar](#)] [[Publisher Link](#)]
- [13] Adel A. Bahaddad et al., "Metaheuristics with Deep Learning-Enabled Parkinson's Disease Diagnosis and Classification Model," *Journal of Healthcare Engineering*, vol. 2022, pp. 1-14, 2022. [[CrossRef](#)] [[Google Scholar](#)] [[Publisher Link](#)]
- [14] Puppala Praneeth et al., "Classification of Parkinson's Disease in Brain MRI Images Using Deep Residual Convolutional Neural Network (DRCNN)," *International Journal of Computer Information Systems and Industrial Management Applications*, vol. 15, pp. 383-395, 2023. [[Google Scholar](#)] [[Publisher Link](#)]
- [15] Feng Chen, Chunyan Yang, and Mohammad Khishe, "Diagnose Parkinson's Disease and Cleft Lip and Palate Using Deep Convolutional Neural Networks Evolved by Ip-Based Chimp Optimization Algorithm," *Biomedical Signal Processing and Control*, vol. 77, 2022. [[CrossRef](#)] [[Google Scholar](#)] [[Publisher Link](#)]
- [16] S. Pragadeeswaran, and S. Kannimuthu, "An Adaptive Intelligent Polar Bear (AIPB) Optimization-Quantized Contempo Neural Network (QCNN) Model for Parkinson's Disease Diagnosis using Speech Dataset," *Biomedical Signal Processing and Control*, vol. 87, no. 2, 2024. [[CrossRef](#)] [[Google Scholar](#)] [[Publisher Link](#)]
- [17] S. Sharanyaa, M. Sambath, and P. N. Renjith, "Optimized Deep Learning for the Classification of Parkinson's Disease Based on Voice Features," *Critical Reviews™ in Biomedical Engineering*, vol. 50, no. 5, 2022. [[Google Scholar](#)] [[Publisher Link](#)]
- [18] Huimin Lu et al., "A Novel Feature Extraction Method Based on Dynamic Handwriting for Parkinson's Disease Detection," *PloS One*, vol. 20, no. 1, pp. 1-26, 2025. [[CrossRef](#)] [[Google Scholar](#)] [[Publisher Link](#)]
- [19] Babita Majhi et al., "An Improved Method for Diagnosis of Parkinson's Disease Using Deep Learning Models Enhanced with Metaheuristic Algorithm," *BMC Medical Imaging*, vol. 24, no. 1, pp. 1-20, 2024. [[CrossRef](#)] [[Google Scholar](#)] [[Publisher Link](#)]
- [20] Shraddha Jain, and Rajeev Srivastava, "Electroencephalogram (EEG) Based Fuzzy Logic and Spiking Neural Networks (FLSNN) for Advanced Multiple Neurological Disorder Diagnosis," *Brain Topography*, vol. 38, 2025. [[CrossRef](#)] [[Google Scholar](#)] [[Publisher Link](#)]
- [21] Siamak Hadadi, and Soodabeh Poorzaker Arabani, "A Novel Approach for Parkinson's Disease Diagnosis Using Deep Learning and Harris Hawks Optimization Algorithm with Handwritten Samples," *Multimedia Tools and Applications*, vol. 83, pp. 81491-81510, 2024. [[CrossRef](#)] [[Google Scholar](#)] [[Publisher Link](#)]
- [22] S. Kumar Reddy Mallidi, and Rajeswara Rao Ramisetty, "Bowerbird Courtship-Inspired Feature Selection for Efficient High-Dimensional Data Analysis Using a Novel Meta-Heuristic," *Discover Computing*, vol. 28, pp. 1-24, 2025. [[CrossRef](#)] [[Google Scholar](#)] [[Publisher Link](#)]
- [23] Aleksa Cuk et al., "Tuning Attention based Long-Short Term Memory Neural Networks for Parkinson's Disease Detection Using Modified Metaheuristics," *Scientific Reports*, vol. 14, pp. 1-12, 2024. [[CrossRef](#)] [[Google Scholar](#)] [[Publisher Link](#)]
- [24] Serdar Ekinci et al., "Novel Application of Sinh Cosh Optimizer for Robust Controller Design in Hybrid Photovoltaic-Thermal Power Systems," *Scientific Reports*, vol. 15, pp. 1-14, 2025. [[CrossRef](#)] [[Google Scholar](#)] [[Publisher Link](#)]
- [25] Jelica Cincovic et al., "Neurodegenerative Condition Detection Using Modified Metaheuristic for Attention Based Recurrent Neural Networks and Extreme Gradient Boosting Tuning," *IEEE Access*, vol. 12, pp. 26719-26734, 2024. [[CrossRef](#)] [[Google Scholar](#)] [[Publisher Link](#)]

- [26] K.V. Siva Prasad Reddy, and Meera Selvakumar, "Personalized Recommendation System to Handle Skin Cancer at Early Stage Based on Hybrid Model," *Network: Computation in Neural Systems*, pp.1-40, 2025. [[CrossRef](#)] [[Google Scholar](#)] [[Publisher Link](#)]
- [27] Aktham Sawan et al., "Hybrid Deep Learning and Metaheuristic Model Based Stroke Diagnosis System Using Electroencephalogram (EEG)," *Biomedical Signal Processing and Control*, vol. 87, no. 1, 2024. [[CrossRef](#)] [[Google Scholar](#)] [[Publisher Link](#)]
- [28] Andrei M. Tudose et al., "Increasing Distributed Generation Hosting Capacity Based on a Sequential Optimization Approach Using an Improved Salp Swarm Algorithm," *Mathematics*, vol. 12, no. 1, pp. 1-21, 2024. [[CrossRef](#)] [[Google Scholar](#)] [[Publisher Link](#)]
- [29] Majdi Mafarja et al., "Classification Framework for Faulty-Software Using Enhanced Exploratory Whale Optimizer-Based Feature Selection Scheme and Random Forest Ensemble Learning," *Applied Intelligence*, vol. 53, pp. 18715-18757, 2023. [[CrossRef](#)] [[Google Scholar](#)] [[Publisher Link](#)]
- [30] D. V. Manjunatha et al., "An Enhanced Video Compression Approach through RLAH Encoding and KDENN Algorithms," *EURASIP Journal on Advances in Signal Processing*, vol. 2024, pp. 1-19, 2024. [[CrossRef](#)] [[Google Scholar](#)] [[Publisher Link](#)]
- [31] Asmaa M. Khalid et al., "A New Binary Object-Oriented Programming Optimization Algorithm for Solving High-Dimensional Feature Selection Problem," *Alexandria Engineering Journal*, vol. 85, pp.72-85, 2023. [[CrossRef](#)] [[Google Scholar](#)] [[Publisher Link](#)]